

Reinforcement Learning for Maneuver Design in UAV-Enabled NOMA System with Segmented Channel

Yuwei Huang, Xiaopeng Mo, Jie Xu, *Member, IEEE*, and Ling Qiu, *Member, IEEE*

Abstract—This letter considers an unmanned aerial vehicle (UAV)-enabled uplink non-orthogonal multiple-access (NOMA) system, where multiple mobile users on the ground send independent messages to a UAV in the sky via NOMA transmission. Our objective is to design the UAV dynamic maneuver for maximizing the sum-rate throughput of all mobile ground users over a finite time horizon. Different from the conventional designs based on deterministic channel (e.g., line-of-sight (LoS) channel) or stochastic channel (e.g., probabilistic LoS channel), we consider a practical segmented channel model, and the UAV is assumed to only know the users' (moving) locations and channel state information (CSI) at the current time slot, but does not have such knowledge for future slots. Under this setup, the dynamic maneuver design problem is very challenging to solve. To tackle this problem, we first propose a new approach for UAV dynamic maneuver design based on reinforcement learning (RL) via Q-learning. Then, in order to speed up the convergence and further improve the throughput, we propose a novel enhanced RL approach by exploiting expert knowledge of well-established wireless channel models to initialize the Q-table values. Numerical results show that our proposed RL and enhanced RL approaches significantly improve the sum-rate throughput, as compared to the conventional maneuver design based on average channel models, and the proposed enhanced RL approach speeds up the learning process.

Index Terms—Unmanned aerial vehicle (UAV), dynamic maneuver design, segmented channel, reinforcement learning (RL), enhanced RL, Q-learning, non-orthogonal multiple-access (NOMA).

I. INTRODUCTION

Unmanned aerial vehicle (UAV)-enabled wireless communications have emerged as one of key technologies for fifth-generation (5G) and beyond wireless networks, where UAVs are employed as aerial wireless platforms (such as relays and base stations (BSs)) to serve end users on the ground [1]. By exploiting the UAVs' fully controllable mobility, the quasi-stationary UAV's placement optimization [2], [3] and the mobile UAV's trajectory optimization [4]–[7] have been studied in the literature in recent years.

Despite the recent research progress, existing works have assumed that the UAV knows the ground users' *static* locations, and can predict the channel state information (CSI) over time based on the assumption that the UAV-to-ground channels follow deterministic channels (e.g., line-of-sight (LoS)

channel) [2]–[6] or stochastic channels (e.g., probabilistic LoS channel) [7]. Nevertheless, for practical scenarios, the ground users may move randomly over time, such that the UAV may not know their locations and CSI over time prior to communication. Thus, how to design the UAV's dynamic maneuver by taking into account the ground users' mobility is a challenging problem that is not well addressed yet.

In particular, motivated by the great success of non-orthogonal multiple-access (NOMA) in 5G, this letter studies a UAV-enabled uplink NOMA system, where multiple *mobile* users on the ground send independent messages to a UAV in the sky via NOMA transmission. Different from prior works considering LoS [2]–[6] or probabilistic LoS channels [7], we consider a practical segmented channel [8]. Under this setup, we design the UAV's dynamic maneuver to maximize the sum-rate throughput of all mobile users over a finite time horizon, subject to practical constraints on the UAV's initial location and flight speed. It is assumed that the UAV only knows the users' (moving) locations and CSI at the current time slot, but does not have such knowledge for future slots. As a result, this problem becomes challenging to solve. To tackle this problem, we adopt the reinforcement learning (RL), a powerful technique of machine learning [9], which can solve sequential decision problems without requiring any knowledge on the environment. First, we propose a new approach to design the UAV dynamic maneuver based on RL by utilizing Q-learning. Then, we propose a novel enhanced RL approach to speed up the convergence by exploiting the well-established wireless channel models as expert knowledge to help initialize Q-table values. Finally, numerical results show that our proposed RL and enhanced RL approaches achieve significant throughput gains over the conventional maneuver design based on average channel models, and the enhanced RL considerably improves the convergence speed.

Notice that RL has attracted growing attentions in UAV-enabled wireless communications [10]–[12], however, to our best knowledge, its application in designing UAV dynamic maneuver under practical segmented channel model by considering the mobility of ground users is new and has not been investigated yet.

II. SYSTEM MODEL

In this letter, we consider the uplink NOMA transmission in a UAV-enabled wireless communication system, in which a set $\mathcal{K} \triangleq \{1, \dots, K\}$ of $K > 1$ mobile users on the ground send

Y. Huang and L. Qiu are with the School of Information Science and Technology, University of Science and Technology of China, Hefei, Anhui, 230027, China (e-mail: hyw1023@mail.ustc.edu.cn, lqiu@ustc.edu.cn).

X. Mo and J. Xu are with the School of Information Engineering, Guangdong University of Technology, Guangzhou, 510006, China (e-mail: xiaopengmo@mail2.gdut.edu.cn, jiexu@gdut.edu.cn). J. Xu is the corresponding author.

independent messages to a UAV flying in the sky. We focus on a finite period $\mathcal{T} = [0, T]$ with duration $T > 0$, which are discretized into N slots each with identical duration $\delta = T/N$. Here, δ is chosen to be sufficiently small such that the UAV's location can be assumed to be approximately constant within each time slot even at its maximum flying speed. We denote $\mathcal{N} \triangleq \{1, \dots, N\}$.

We consider a three-dimensional (3D) Cartesian coordinate system, where each user k has a zero altitude and moves slowly over time. Let $\mathbf{w}_k[n] = (x_k[n], y_k[n])$ denote the horizontal location of user k at slot $n \in \mathcal{N}$. The UAV flies at a fixed altitude $H > 0$ in meter (m) with the time-varying horizontal location being $\mathbf{q}[n] = (x[n], y[n])$ at slot $n \in \mathcal{N}$. Suppose that the UAV's initial horizontal location is pre-determined as $\hat{\mathbf{q}}_I = (x_I, y_I)$, and thus we have $\mathbf{q}[1] = \hat{\mathbf{q}}_I$. At each slot $n \in \mathcal{N}$, the UAV can change its location or hover at the same location. For ease of analysis, we define $\tilde{\mathcal{A}} = \{(0, 0), (-\lambda, 0), (\lambda, 0), (0, \lambda), (0, -\lambda)\}$ as the set of UAV's possible location changes over one slot, each element of which corresponds to static hovering, flying left, right, forwards, and backwards, respectively. Here, λ is a constant denoting the UAV's displacement at each slot. Let $\boldsymbol{\lambda}[n]$ denote the UAV's location change at each slot n . We thus have $\boldsymbol{\lambda}[n] \in \tilde{\mathcal{A}}$ and $\mathbf{q}[n] = \mathbf{q}[n-1] + \boldsymbol{\lambda}[n-1]$, $\forall n \in \mathcal{N} \setminus \{1\}$.

Different from conventional designs based on LoS or probabilistic LoS channels, in this letter, we consider a practical segmented channel model as in [8], in which if there are obstacles between the UAV and the user k , the channel follows a non-line-of-sight (NLoS) model, and otherwise, the channel follows a LoS channel. Thus, the channel power gain from the user k to the UAV is denoted by $h_{k,b}[n] = \mu_{k,b}[n]\xi_{k,b}[n]\beta_{k,b}[n]d_k[n]^{-\alpha_{k,b}[n]}$, where $\alpha_{k,b}[n]$ is the path loss exponent, $\beta_{k,b}[n]$ is the reference channel power gain, $\xi_{k,b}[n]$ denotes the shadowing component, $\mu_{k,b}[n]$ accounts the small-scale fading, and $b \in \{\text{LoS}, \text{NLoS}\}$ represents the strong dependence of the propagation parameters on LoS or NLoS scenario. In the following, we drop the subscript b for ease of exposition.

We consider the uplink NOMA transmission over the multiple-access channel (MAC) from the K users to the UAV. At slot $n \in \mathcal{N}$, let $u_k[n]$ denote the message (with unit power) transmitted by each user $k \in \mathcal{K}$. Accordingly, the received signal at the UAV is given by $\tilde{s}[n] = \sum_{k \in \mathcal{K}} \sqrt{\tilde{P}h_k[n]}u_k[n] + v[n]$, where \tilde{P} is the fixed transmit power of user k , and $v[n]$ denotes the additive white Gaussian noise (AWGN) at the UAV receiver with noise power σ^2 . To achieve the capacity region of MAC, the UAV adopts the successive interference cancellation (SIC) to decode the information [13], and then the K users can employ Gaussian signaling with $u_k[n]$'s being independent circularly symmetric complex Gaussian (CSCG) random variables with zero mean and unit variance. Specifically, at each time slot n , denote $\varphi = [\varphi(1), \dots, \varphi(K)]$ as the decoding order at the UAV, which indicates that the UAV receiver first decodes the message $u_{\varphi(K)}[n]$ from user $\varphi(K)$, then decodes $u_{\varphi(K-1)}[n]$ by cancelling the interference from $u_{\varphi(K)}[n]$, followed by $u_{\varphi(K-2)}[n], u_{\varphi(K-3)}[n]$, and so on, until $u_{\varphi(1)}[n]$. Therefore,

under any given φ , the achievable rate by user $\varphi(k)$ at each slot n in bits/second/Hertz (bps/Hz) is given by

$$r_{\varphi(k)}[n] = \log_2 \left(\frac{\sum_{j=1}^k \tilde{P}h_{\varphi(j)}[n] + \sigma^2}{\sum_{i=1}^{k-1} \tilde{P}h_{\varphi(i)}[n] + \sigma^2} \right), \forall k \in \mathcal{K}.$$

As a result, the K users' sum-rate throughput at each slot n is expressed as follows, which is irrelevant to the decoding order φ [13].

$$\tilde{R}[n] = \sum_{k \in \mathcal{K}} r_{\varphi(k)}[n] = \log_2 \left(1 + \tilde{P} \sum_{k \in \mathcal{K}} h_k[n]/\sigma^2 \right). \quad (1)$$

Our objective is to maximize the average sum-rate throughput of all ground users over the duration- N period (i.e., $\frac{1}{N} \sum_{n=1}^N \tilde{R}[n]$), by optimizing the UAV's dynamic maneuver $\{\mathbf{q}[n]\}$. Thus, the problem of our interest is formulated as

$$\begin{aligned} \text{(P1):} \quad & \max_{\{\mathbf{q}[n], \boldsymbol{\lambda}[n] \in \tilde{\mathcal{A}}\}} \frac{1}{N} \sum_{n=1}^N \log_2 \left(1 + \tilde{P} \sum_{k \in \mathcal{K}} h_k[n]/\sigma^2 \right) \\ & \text{s.t. } \mathbf{q}[1] = \hat{\mathbf{q}}_I \\ & \mathbf{q}[n] = \mathbf{q}[n-1] + \boldsymbol{\lambda}[n-1], \forall n \in \mathcal{N} \setminus \{1\}, \end{aligned} \quad (2)$$

(3)

where (2) and (3) denote UAV's initial location and maneuver constraints, respectively. It is assumed that to achieve the data-rate throughput at each slot n , the UAV is able to know the users' locations and CSI at the current time slot by using proper localization and channel estimation algorithms; however, the UAV does not know the users' locations and CSI for future slots due to their random mobility. Thus, prior to communication, the UAV is not aware of the CSI $\{h_k[n]\}$ over time, and accordingly does not know the objective function of (P1). In this case, problem (P1) is challenging to solve.

III. PROPOSED SOLUTION TO (P1)

In this section, we first propose a novel approach to solve (P1) based on RL by using Q-learning, and then propose a novel enhanced RL approach to help speed up the convergence and further improve the throughput, in which the wireless models are utilized as expert knowledge to help initialize the values of Q-table.

A. RL for UAV Maneuver Design

Before proceeding, we briefly introduce RL and Q-learning. RL is an area of machine learning, which studies how an agent can take actions in an environment to maximize the cumulative reward over a certain time horizon [9]. Q-learning is a specific RL method, which enables the agent to find an optimal policy for reward maximization, via updating a Q-table that returns the expected rewards under different actions.

In particular, we describe the Q-learning based on a Markov decision process (MDP) $\{\mathcal{S}, \mathcal{A}, P, R\}$ with state space \mathcal{S} , action space \mathcal{A} , state transition probability $P_a(s, s') = Pr(s_{n+1} = s' | s_n = s, a_n = a)$, and reward function $R_a(s, s')$. At each step n , the agent observes its current state s_n , selects and performs an action $a_n \in \mathcal{A}$, then moves into the subsequent state s_{n+1} and receives an immediate

reward $r_n = R_{a_n}(s_n, s_{n+1})$. In general, the goal of the agent is to determine a policy π to maximize the received reward, where the policy is defined as $\pi(a|s) = Pr(a_n = a|s_n = s)$. Then, define the Q-function (or state-action value function) as the expected discounted reward for executing action a at state s based on π . Thus, for policy π , the Q-function is given by

$$Q^\pi(s, a) = \mathbb{E}_\pi\{R_n|s_n = s, a_n = a\}, \quad (4)$$

where $\mathbb{E}\{\cdot\}$ denotes the statistic expectation, and

$$R_n = \sum_{i=0}^{N-1} \gamma^i R_{n+i+1} \quad (5)$$

denotes the discounted sum of all future rewards at current step n , with $\gamma \in [0, 1)$ denoting the discount factor to balance the tradeoff between long-term and short-term rewards. Particularly, $\gamma \rightarrow 1$ represents that the agent focuses on the long-term reward, while $\gamma \rightarrow 0$ denotes that the agent only considers the immediate reward. Accordingly, the agent's objective becomes to find an optimal policy to maximize the Q-function, i.e., $\pi^*(a|s) = \arg \max_{a \in \mathcal{A}} Q^{\pi^*}(s, a)$ ¹. Notice that if the optimal policy π^* is not unique, then we can simply choose any one of these policies without loss of optimality. By combining (4) and (5), the Q-table can be updated in each step n as

$$Q^\pi(s_n, a_n) = Q^\pi(s_n, a_n) + \alpha(r_n + \gamma \max_a Q^\pi(s_{n+1}, a) - Q^\pi(s_n, a_n)), \quad (6)$$

where $\alpha \in [0, 1]$ denotes the learning rate to determine how much the old information is retained. To ensure the convergence of Q-learning, the learning parameters α and γ should be chosen properly.

Now, we explain how to use RL to solve (P1) with implicit objective functions based on Q-learning. Specifically, we use a Q-table to approximate the Q-functions, and set the state space as $\mathcal{S} = \{\mathbf{q}[n]\}$ for each slot n and the action space as $\mathcal{A} = \tilde{\mathcal{A}}$. Then, the RL-based solution proceeds as follows.

Consider any one particular slot $n \in \mathcal{N}$, where the UAV stays at location $\mathbf{q}[n]$ with current state $s_n = \mathbf{q}[n]$. In this case, the UAV chooses an action (location change) $a_n = \lambda[n] \in \mathcal{A}$ by employing the ϵ -greedy policy based on the Q-table, such that the UAV chooses a random action within \mathcal{A} with probability $\epsilon \in [0, 1]$, and chooses the action that maximizes the Q-function, i.e., $a = \arg \max_{\tilde{a} \in \mathcal{A}} Q(s_n, \tilde{a})$, with probability $1 - \epsilon$. Based on this action, the UAV then moves to a new location $\mathbf{q}[n+1] = \mathbf{q}[n] + \lambda[n]$ (corresponding to the subsequent state s_{n+1}), and receives an immediate reward as the instantaneous sum-rate throughput $\tilde{R}[n]$ in (1), i.e., $r_n = R_{a_n}(s_n, s_{n+1}) = \tilde{R}[n]$. Next, the current Q-value, i.e., $Q^\pi(s_n, a_n)$, is updated according to (6). The above procedure proceeds until $n = N$. By properly choosing the parameter ϵ , the UAV can efficiently balance the trade-off between exploring untried locations (states) to get more experiences versus exploiting already tried locations to gain higher rewards, which is referred to as the *exploration-exploitation trade-off* in RL literature [9]. In general, ϵ should be chosen to be exponentially decreasing over time. Furthermore, in

our considered dynamic environment with mobile users, the discount factor should be chosen to focus on the long-term reward, i.e., $\gamma \rightarrow 1$.

The practical implementation of Q-learning critically depends on the initial Q-table at slot $n = 1$. In our proposed RL-based design, the initial Q-table values are set to zero similar as [10]. However, it generally takes a long time to converge towards the optimal solution, which may considerably compromise the overall throughput performance during the whole communication period of interest.

B. Enhanced RL for UAV Maneuver Design

To tackle the slow convergence issue of the RL-based design, in this subsection we propose a novel enhanced RL approach by exploiting wireless expert information to aid Q-learning. In the following, we first explain how to roughly predict the CSI and estimate rate functions by using expert information, and then add a procedure to properly initialize the Q-table based on such estimations.

In the wireless communications society, there have been well-established models on wireless channels and communication rates, which have been overlooked in the above proposed RL-based approach. Based on this observation, we propose to exploit such knowledges to help initialize the Q-table. More specifically, based on the rate function in (1) under NOMA transmission, it is evident that we can (roughly) estimate the communication rate over time based on only coarse channel information. Though we do not know the exact channel environment and CSI, we know that any wireless channels generally follow a simplified stochastic model with path loss, shadowing, and small-scale fading [13]. In addition, for UAV-to-ground communications, we additionally know that the channel power gain is dependent on the elevation angle, which can be characterized by the LoS probability in an average/stochastic sense². In this case, we can use the average channel power gain as a rough channel prediction, i.e., [14]

$$\bar{h}_k[n] = p_{k,\text{LoS}}[n] \bar{\beta} d_k[n]^{-\bar{\alpha}} + \eta(1 - p_{k,\text{LoS}}[n]) \bar{\beta} d_k[n]^{-\bar{\alpha}}, \quad (7)$$

where $p_{k,\text{LoS}}[n] = 1/(1 + C \exp(-D(\arcsin(H/d_k[n]) - C)))$ is the LoS probability for the link between the UAV and user k with C and D being the probability parameters, $\bar{\beta}$ is the average reference channel power gain over all user-UAV links, $\bar{\alpha}$ is the average path loss exponent over all user-UAV links, and $\eta < 1$ is an additional attenuation factor due to the NLoS propagation. Note that although the parameters C , D , η , $\bar{\beta}$, and $\bar{\alpha}$ are not known by the UAV, their values are limited within certain ranges based on empiric results (as explained in Section IV). Thus, we properly choose these parameters for getting rough channel predictions. In the special case with LoS UAV-to-ground channels, we have $p_{k,\text{LoS}}[n] = 1, \forall k \in \mathcal{K}, n \in \mathcal{N}$, which becomes an accurate channel model (instead of stochastic) and is widely used in UAV maneuver design [2]–[6].

¹In practical implementation, the agent may need to act randomly with a certain probability for exploring unknown states, as explained in detail later.

²Notice that the probabilistic LoS model can only reveal the stochastic property of UAV-to-ground channels over a certain area. For any specific link, the wireless channel can either be LoS or non-line-of-sight (NLoS).

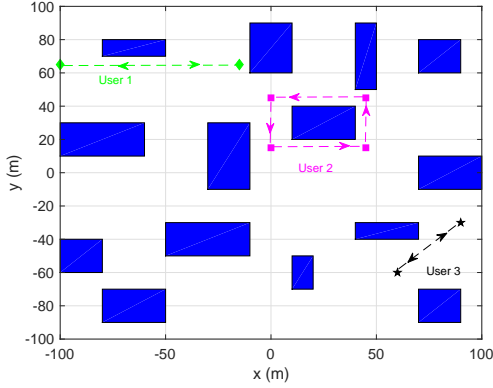


Fig. 1. Simulation setup with blue cubes denoting obstacles (e.g., buildings).

Based on such rough channel prediction models, we estimate the initial values of Q-table by adding additional training procedure, which is implemented similarly as that in the proposed RL-based approach in Section III-A. The only difference is that during the training procedure, the UAV computes the rewards by using the above rough channel estimations in (7) based on the users' initial locations (as we cannot predict their movement). After convergence, the training procedure obtains a Q-table that will be used as the initial one for the proposed RL-based approach in Section III-A. If the adopted "average" channel model perfectly matches with the real environment (with static users), the obtained Q-table is generally optimal. Even if it does not match in practical scenarios with mobile users and time-varying environment, the obtained-initial Q-table can still give rough information about the achievable rewards (throughputs) at different UAV locations, thus helping speed up the convergence of the subsequent Q-learning, as will be shown next in simulations.

IV. NUMERICAL RESULTS

In this section, we present numerical results to validate the performance of our proposed RL and enhanced RL approaches. Unless otherwise stated, we set the users' transmit power as $P = 23$ dBm, the UAV's fixed flight altitude as $H = 100$ m, and the noise power as $\sigma^2 = -80$ dBm. Then, we consider an $200 \text{ m} \times 200 \text{ m}$ area with $K = 3$ mobile users, as shown in Fig. 1, where the blue cubes denote obstacles (e.g., buildings) with height 40 m. For the considered practical segmented channel model, we use Rician fading to model the small-scale fading, and set $\beta_{k,\text{NLoS}}[n] = -40$ dB, $\beta_{k,\text{LoS}}[n] = -30$ dB, $\alpha_{k,\text{NLoS}}[n] = 4$, $\alpha_{k,\text{LoS}}[n] = 2$, $10 \log_{10}(\xi_{k,\text{NLoS}}[n]) \sim \mathcal{N}(0, 5)$, and $10 \log_{10}(\xi_{k,\text{LoS}}[n]) \sim \mathcal{N}(0, 2)$, where \mathcal{N} denotes the Gaussian distribution. The UAV's initial location is set as $\hat{q}_I = (-95 \text{ m}, -95 \text{ m})$. To implement the Q-learning, we divide the whole area into 20 by 20 grid, and set the UAV's displacement at each slot as $\lambda = 10$ m. During the Q-learning, if the UAV's action leads to a location outside the 20 by 20 grid, we will add an additional negative reward. The learning rate is set as $\alpha = 0.3$, the discount factor is set as $\gamma = 0.9$ to make the UAV focus on long-term reward, and the probability for random actions ϵ is decreasing over time from the initial

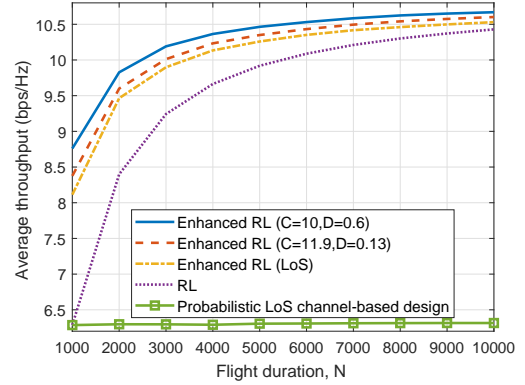


Fig. 2. Throughput comparison among enhanced RL, RL, and probabilistic LoS channel-based approaches.

value of $\epsilon = 0.9$. Furthermore, for the probabilistic LoS channel used in additional training procedure of enhanced RL approach³, we set $\bar{\alpha} = 2.3$, $\bar{\beta} = -30$ dB, and $\eta = 0.1$. For comparison, we consider the following maneuver design based on conventional probabilistic LoS channel.

Probabilistic LoS channel-based maneuver design: The UAV optimizes its action by assuming the channels to be probabilistic LoS channel. At slot $n \in \mathcal{N}$, the UAV knows the current user locations and solves the following sum-rate maximization problem:

$$(P2.n): \max_{\mathbf{q}[n]} \log_2 \left(1 + \sum_{k=1}^K \frac{P \bar{h}_k[n]}{\sigma^2} \right).$$

The optimal solution to (P2.n), denoted as $\tilde{\mathbf{q}}^*[n]$, can be obtained via a two-dimensional search in this area. Accordingly, the UAV chooses $\lambda[n] \in \tilde{\mathcal{A}}$ such that it moves towards $\tilde{\mathbf{q}}^*[n]$.

Fig. 2 shows the average throughput of our proposed designs. First, it is observed that RL-based designs significantly outperform the probabilistic LoS channel-based design. This is because the UAV-to-ground channels are NLoS with high probability due to the obstacles, which mismatch with the adopted probabilistic LoS channel model, thus leading to compromised performance for the probabilistic LoS channel-based approach. Next, the enhanced RL designs are observed to outperform the RL design, especially when the flight duration is small. This is because that the enhanced designs exploit the well-established wireless models as the expert knowledge to help initialize the Q-table to give rough information about the achievable rewards at different UAV locations, rather than setting all initial values of Q-table to zero as in the RL design. The performance gain indicates the significance of exploiting wireless expert knowledge to aid RL in speeding up the convergence. Finally, it is observed that the performance of enhanced RL designs highly depends on the adopted channel models for training procedure. In particular, using the probabilistic LoS models is observed to achieve higher throughput than the LoS model. This demonstrates that employing a model

³In general, if we roughly know some statistical information about the areas (e.g., the intensity of buildings), we can choose channel parameters that are mostly suitable for this area. Otherwise, we choose these parameters randomly.

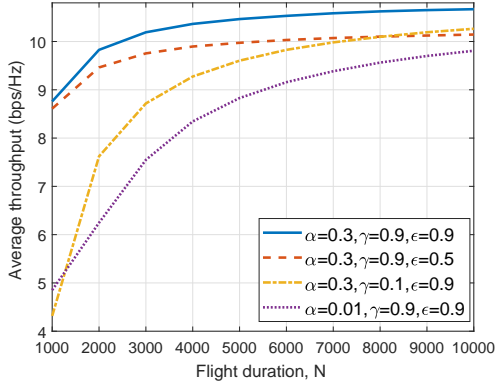


Fig. 3. Throughput comparison under different learning parameters.

that matches well with practical environment is essential for the enhanced RL designs.

Fig. 3 shows the average throughput of the enhanced RL design under different learning parameters, with $C = 10$ and $D = 0.6$ for the employed probabilistic LoS channel model. In our setup, it is observed that using $\alpha = 0.3$, $\gamma = 0.9$, and $\epsilon = 0.9$ achieves higher throughput than other parameters. This indicates the importance of choosing proper learning parameters in RL.

V. CONCLUSIONS

This letter considered the UAV-enabled uplink NOMA system to maximize the sum-rate throughput of all users over a finite horizon, subject to practical constraints on the UAV's initial location and flight speed. We considered the practical segmented channel model and assumed that the UAV did not know any information about the channel environment and users' movement *a priori*. We proposed a novel approach to design the UAV maneuver based on RL via Q-learning, and building upon it we further proposed an enhanced RL approach, in which the wireless expert information on UAV-to-ground channel was utilized to facilitate the Q-learning via adding additional training procedure. Numerical results showed that our proposed RL-based designs significantly outperformed the conventional maneuver design based on average channel power gains, and the enhanced RL approach improved the convergence speed significantly as compared to the RL approach.

REFERENCES

- [1] Y. Zeng, R. Zhang, and T. J. Lim, "Wireless communications with unmanned aerial vehicles: Opportunities and challenges," *IEEE Commun. Mag.*, vol. 54, no. 5, pp. 36–42, May 2016.
- [2] J. Lyu, Y. Zeng, R. Zhang, and T. J. Lim, "Placement optimization of UAV-mounted mobile base stations," *IEEE Commun. Lett.*, vol. 21, no. 3, pp. 604–607, Mar. 2017.
- [3] P. Li and J. Xu, "Placement optimization for UAV-enabled wireless networks with multi-hop backhauls," *J. Commun. Inf. Netw.*, vol. 3, no. 4, pp. 64–73, Dec. 2018.
- [4] Y. Zeng, R. Zhang, and T. J. Lim, "Throughput maximization for UAV-enabled mobile relaying systems," *IEEE Trans. Commun.*, vol. 64, no. 12, pp. 4983–4996, Dec. 2016.
- [5] J. Xu, Y. Zeng, and R. Zhang, "UAV-enabled wireless power transfer: trajectory design and energy optimization," *IEEE Trans. Wireless Commun.*, vol. 17, no. 8, pp. 5092–5106, May 2018.

- [6] Q. Wu, J. Xu, and R. Zhang, "Capacity characterization of UAV-enabled two-user broadcast channel," *IEEE J. Sel. Areas Commun.*, vol. 36, no. 9, pp. 1955–1971, Sep. 2018.
- [7] M. Mozaffari, W. Saad, M. Bennis, and M. Debbah, "Mobile unmanned aerial vehicles (UAVs) for energy-efficient Internet of things communication," *IEEE Trans. Wireless Commun.*, vol. 16, no. 11, pp. 7574–7589, Nov. 2017.
- [8] J. Chen and D. Gesbert, "Optimal positioning of flying relays for wireless networks: A LOS map approach," in *Proc. IEEE ICC*, Jul. 2017.
- [9] R. S. Sutton and A. G. Barto, *Introduction to Reinforcement Learning*, 2nd ed. Cambridge, Massachusetts: MIT Press, 2017.
- [10] H. Bayerlein, P. D. Kerret, and D. Gesbert, "Trajectory optimization for autonomous flying base station via reinforcement learning," in *Proc. IEEE SPAWC*, Jun. 2018.
- [11] Y. Liu, Z. Qin, Y. Cai, Y. Gao, G. Ye, Li, and A. Nallanathan, "UAV communication based on non-orthogonal multiple access," *IEEE Wireless Commun.*, vol. 26, no. 1, pp. 52–57, Feb. 2019.
- [12] U. Challita, W. Saad, and C. Bettstetter, "Interference management for cellular-connected UAVs: A deep reinforcement learning approach," *IEEE Trans. Wireless Commun.*, vol. 18, no. 4, pp. 2125–2140, Apr. 2019.
- [13] David. T and P. Viswanath, *Fundamentals of Wireless Communication*, Cambridge University press, 2005.
- [14] A. Al-Hourani, S. Kandeepan, and S. Lardner, "Optimal LAP altitude for maximum coverage," *IEEE Wireless Commun. Lett.*, vol. 3, no. 6, pp. 569–572, Dec. 2014.